Physiol. Res. 65: 597-608, 2016

Analysis of Expression Profiles of Genes Involved in F_oF_1-ATP Synthase Biogenesis During Perinatal Development in Rat Liver and Skeletal Muscle

J. SPÁČILOVÁ[1], M. HŮLKOVÁ[1], A. HRUŠTINCOVÁ[1], V. ČAPEK[1], M. TESAŘOVÁ[1], H. HANSÍKOVÁ[1], J. ZEMAN[1]

[1]Laboratory for Study of Mitochondrial Disorders, Department of Pediatrics and Adolescent Medicine, First Faculty of Medicine, Charles University in Prague and General University Hospital in Prague, Prague, Czech Republic

Received July 9, 2015
Accepted November 12, 2015
On-line March 15, 2016

Summary

During the process of intra-uterine mammalian fetal development, the oxygen supply in growing fetus is low. A rapid switch from glycolysis-based metabolism to oxidative phosphorylation (OXPHOS) must proceed during early postnatal adaptation to extra-uterine conditions. Mitochondrial biogenesis and mammalian mitochondrial F_OF_1-ATP synthase assembly (complex V, EC 3.6.3.14, ATPase) are complex processes regulated by multiple transcription regulators and assembly factors. Using RNA expression analysis of rat liver and skeletal tissue (*Rattus norvegicus*, Berkenhout, 1769), we describe the expression profiles of 20 genes involved in mitochondrial maturation and ATP synthase biogenesis in detail between the 16th and 22nd day of gestation and the first 4 days of life. We observed that the most important expression shift occurred in the liver between the 20th and 22nd day of gestation, indicating that the fetus prepares for birth about two days before parturition. The detailed mechanism regulating the perinatal adaptation process is not yet known. Deeper insights in perinatal physiological development will help to assess mitochondrial dysfunction in the broader context of cell metabolism in preterm newborns or neonates with poor adaptation to extra-uterine life.

Key words

ATP synthase • Fetal development • Mitochondrial biogenesis • Rat liver • Skeletal muscle

Corresponding author

J. Zeman, Department of Pediatrics and Adolescent Medicine, First Faculty of Medicine, Charles University in Prague, General University Hospital in Prague, Ke Karlovu 2, 128 08 Prague 2, Czech Republic.

Fax: +420 224 96 7099. E-mail: jzem@lf1.cuni.cz

Introduction

Mitochondria are important organelles in the mammalian cell due to their role in the synthesis of more than 90 % of cellular ATP by oxidative phosphorylation (OXPHOS). The first four complexes create the electron transport chain, which generates a mitochondrial inner membrane (MIM) potential used by the F_OF_1-ATP synthase (complex V, EC 3.6.3.14, ATPase) to generate ATP (Boyer 1975). In cases of oxidative stress or hypoxia, ATP is hydrolyzed to prevent MIM potential decrease and mitochondrial destabilization. ATPase, an approximately 600 kDa complex consisting of at least 17 subunits, is formed by a F_1 catalytic portion and F_O proton-translocating portion connected by a central and peripheral stalk. Subunits a and A6L are encoded by mtDNA (*mt-Atp6* and *mt-Atp8*); the rest is nDNA-encoded and transported to the mitochondria during translation. ATPase biogenesis is a multi-step process assisted by assembly factors, in mammals by *Atpaf1* and *Atpaf2* (Wang *et al.* 2001) and a specific non-essential assembly factor *Tmem70* (Cízková *et al.* 2008). A summary table of 5 ATPase subunits and the 13 other OXPHOS- or mitochondria-related factors analyzed in

our study is presented in the Supplement (Table S1): nDNA-encoded ATPase structural subunits; mtDNA-encoded ATPase and OXPHOS subunits; ATPase assembly factors and other expression regulators involved in the mechanism of mitochondrial metabolism acceleration.

OXPHOS capacity is highly variable to maintain energy demands in various tissues throughout ontogenetic growth of the organism (Benard *et al.* 2006). In mammals, fetal metabolism is glycolytic (Burch *et al.* 1963). The partial oxygen pressure is low *in utero*, and therefore, OXPHOS capacity is low (Prystowsky 1957). After birth, a rapid mitochondrial maturation occurs and the switch to oxidative metabolism must proceed (Valcarce *et al.* 1988). The concentration of ATP is increased two-fold in the liver of the two-hour-old newborn rat (Sutton and Pollak 1978). Mitochondrial switch to oxidative phosphorylation has been previously reported in various tissues and organisms by an increase in OXPHOS activity or mtDNA amount (Izquierdo and Cuezva 1997, Izquierdo *et al.* 1990, 1995, Minai *et al.* 2008, Pejznochova *et al.* 2010, Pejznochová *et al.* 2008). In various tissues, distinct stoichiometry of the OXPHOS complexes was assessed (Lenaz and Genova 2007, Schägger and Pfeiffer 2001). The pool of electron carriers CoQ10 and cytochrome *c* is generally in excess to complexes III and IV, respectively (Lenaz and Genova 2009). These findings highlight that to establish adequate ATP synthesis machinery in mitochondria, precise regulation of OXPHOS biogenesis is necessary.

Nevertheless, few studies have analyzed the expression of mitochondrial genes during perinatal development. A study reported by Izquierdo *et al.* (1995) shows that levels of OXPHOS transcripts remain unchanged after the first postnatal day and that a key role in prenatal expression regulation is played by 3`UTR region of *ATP5B* mRNA, coding β-F_1-ATPase subunit. Another study describes cytochrome *c* oxidase subunits gene expression increase in skeletal muscle, kidney, brain and heart ventricle, but only postnatally (Kim *et al.* 1995). Broader insight into mitochondrial gene expression changes has been reported in human fetal liver and skeletal muscle mtDNA expression and maintenance (Pejznochova *et al.* 2010), but adequate mapping of mitochondrial biogenesis in perinatal period is missing. Cuezva *et al.* (1997) showed that expression changes proceed at a transcriptional level during fetal development; as shown for only a single transcript expression – β-F_1-ATPase subunit – and its regulator miR-127-5p (Willers *et al.* 2012). Our pilot study describes the orchestration of the mRNA expression of 20 genes important to ATPase biogenesis and mitochondrial oxidative metabolism in liver and muscle tissue during rat perinatal development (*Rattus norvegicus*, Berkenhout, 1769), comparing both late fetal and early postnatal samples using a brief and simple approach for expression data analysis. We decided to apply a broad RNA microarray analysis to find specific interconnections among ATPase subunits and transcription regulators or activators. We believe that these data may later enable identification of another key factors regulating mitochondrial biogenesis, and thus improve diagnostics of inborn metabolic disorders and care of the preterm or low-birth-weight newborns.

Materials and Methods

Ethics

Rat tissues were received in collaboration with the Institute of Physiology, The Czech Academy of Sciences, Prague, where all animals were housed. All experiments with living rats were performed in agreement with the Animal Protection Law of the Czech Republic and were approved by the Ethics Committee of the Institute of Physiology, The Czech Academy of Sciences, Prague.

Tissues

A set of rat liver (n_{liv}=54) and skeletal muscle (n_{mus}=35) fetal and postnatal tissue samples was obtained after sacrifice of pregnant Wistar mothers between the 16th and 22nd gestational days (F16-F22) and Wistar litters between the 1st and 4th postnatal days (P1-P4), respectively. For SDS-PAGE, samples from 5-, 7-, 13-, and 18-day-old (P5, P7, P13, and P18) and adult (P90) animals were obtained. The fetuses were delivered by Caesarean section. All tissues were frozen immediately in liquid nitrogen. For further analyses, all samples were stored at −80 °C.

Biochemical analyses

Tissue homogenization for simultaneous RNA and protein isolation was performed in TriReagent solution (MRC, Ohio, USA) using an ULTRA-TURRAX T8 homogenizer (IKA, Germany) according to the manufacturer's protocol.

Protein concentration was determined by the method of Lowry *et al.* (1951).

Tricine SDS/PAGE and Western blot (Schägger and von Jagow 1987) was carried out under standard conditions with 12 % polyacrylamide and 4 % (w/v) SDS gels. Samples were dissolved in sample buffer (50 mM Tris/HCl (pH 6.8), 12 % (v/v) glycerol, 4 % SDS, 2 % (v/v) 2-mercaptoethanol and 0.01 % (w/v) Bromophenol Blue for 30 min at 37 °C; 20 μg of sample protein was loaded for each lane. To choose the reference protein, we tested several proteins commonly used as the "housekeeping" loading controls. We have chosen Hprt as the best reference candidate protein for this type of study, but due to nonzero variability among fetal/postnatal samples we present the data as the relative ratio Atp5/Hprt. To analyze the protein content of the Atp5a subunit and reference Hprt protein, gels were electroblotted on Immobilon™-P PVDF membranes (Millipore, Massachusetts, USA) as previously described (Fornuskova *et al.* 2008). Primary detection of the blots was performed with mouse monoclonal antibodies against Atp5a and Hprt (Abcam, Cambridge, UK; Atp5a ab110273, Hprt ab109021) at 1:10 000 and 1:20 000 dilutions, respectively. Secondary detection was carried out as described elsewhere (Fornuskova *et al.* 2008). Immunodetected protein signal was quantified by Quantity One software (Bio-rad, California, USA) twice per membrane replicate. The ratio between anti-Atp5a and anti-Hprt signals of control adult rat liver (at the age of 90 days) was set to 100 %. Fetal/early postnatal ratios (average) are shown as a percentage of the control value.

RNA isolation and cDNA reverse transcription

RNA was isolated from each liver and muscle tissue sample by TriReagent solution (MRC, Ohio, USA) according to the manufacturer's protocol. Total RNA was treated by DNase I (Ambion, Massachusetts, USA). The quality and quantity of total RNA was checked using an Agilent Bioanalyzer 2100 (Agilent Technologies, California, USA) and NanoDrop 1000 (Thermo Scientific, Massachusetts, USA). The RNA quality indicator was above 7 for all samples on a scale of 1-10. After preparation, RNA samples were stored at −80 °C until use. 1000 ng of total RNA was transcribed to cDNA using Superscript III Reverse Transcriptase (Invitrogen, Massachusetts, USA) and Oligo-dT primers (Promega, State of Wisconsin, USA). RT-minus controls were prepared (without reverse transcriptase). cDNA was stored at −20 °C until analysis by real-time PCR, but at most for 2 weeks. cDNA was thawed only twice.

Real-time PCR

TaqMan® Gene Expression Assay (25 μl) contained 2 × TaqMan® Gene Expression Master Mix (Applied Biosystems, Massachusetts, USA), 1.25 μl of TaqMan® probe FAM-MGB (Applied Biosystems, Massachusetts, USA; *mt-Atp6* Rn03296710_s1, *Atp5g2* Rn00821711_g1, *Atp5a1* Rn01527025_m1, *Atp5o* Rn00756345_m1, *Psmb6* Rn00821581_g1, *Hprt* Rn01527840_m1) and 1 μl cDNA template. Each cDNA sample was diluted so that 1 μl of cDNA correspond to 25 ng of total RNA used for reverse transcription. Thermal-cycling conditions were specified according to the manufacturer`s protocol. To assess the reaction efficiency of each probe (between 0.9 and 1.1), a calibration curve was performed with control sample dilutions 100, 50, 25, 12.5 and 6.25 % of pooled cDNA. Two reference genes were chosen according to expression level quantification. The stability of gene expression was evaluated by GeNorm. *Tbp* and *Psmb6* were the most stably expressed genes in the liver, while *Hprt* and *Psmb6* in the skeletal muscle, similar to what was published earlier (Pejznochova *et al.* 2010). The reaction efficiency and the relative quantification of all genes were calculated in GenEx software. For each gene, the samples were analyzed twice in duplicate. All statistical analyzes were provided by STATISTICA 12.0 (StatSoft, Oklahoma, USA) and R ("R Core Team" URL: http://www.r-project.org/). Depicted illustrative expression curve profiles were obtained when performing least squares regression analysis. Results were considered significant when the corresponding $p \leq 0.05$ (Table 1). Constructed expression plots consisted of at least three samples quantified twice in duplicate, with each dot representing a mean value.

cDNA microarray performance and data analysis

Measurements of genome-wide mRNA expression were conducted using the GeneChip Rat Gene 1.0 ST Arrays (Affymetrix, California, USA), which covers probes for 16 557 well-annotated RefSeq genes. RNA was purified in five developmental days (16th, 20th, and 22nd fetal (F16, F20, F22) and 1st and 4th postnatal (P1, P4)) using an RNeasy Mini Kit (QIAGEN, Germany) before the analysis. Generation of labelled cDNA, hybridizations, and microarray scanning were performed under contract by the Centre for Applied Genomics in the Peter Gilgan Centre for Research and Learning, The Hospital for Sick Children (Toronto,

Table 1. Expression of transcripts selected for validation by qPCR. Significant expression trends are shown in bold (≤0.05). Positive correlation coefficient implies to mRNA level increase, negative to decrease.

	p	Correlation coefficient	n	p	Correlation coefficient	n
	Liver			**Skeletal muscle**		
Atp5g2	**<0.05**	**0.35**	**72**	0.318	−0.18	33
Atp5o	**<0.05**	**0.43**	**72**	0.326	0.18	33
mt-Atp6	**<0.05**	**0.81**	**72**	**<0.05**	**0.41**	**33**
Atpaf2	**<0.05**	**0.44**	**57**	**<0.05**	**−0.51**	**33**
Atp5a1	**<0.05**	**0.45**	**53**	0.97	0.01	33
Tmem70	**<0.05**	**0.63**	**72**	0.585	0.10	33

n – number of analyzed samples

Canada). The data were assessed for quality and subjected to robust multi-array averaging (RMA) normalization (Affymetrix expression console; Affymetrix, California, USA) in R ("R Core Team" URL: http://www.r-project.org/).

Cluster analysis

The dendrogram analysis (clustering) of gene expression was accomplished using the programs STATISTICA 12.0 (Statsoft, Oklahoma, USA) and GenEx (MultiD Analyzes AB, Göteborg, Sweden). The data for genes *Atp5a1, Atp5d, Atp5g2, Atp5o, Atpaf1, Atpaf2, Esrra, Gabpa, Hnf4a, mt-Co1, mt-Co2, mt-Nd2, mt-Nd5, Nrf1, Ppargc1a, Ppargc1b, Pprc1, Tfam, Tmem70* and a probe for set of *mt-Co3/mt-Atp8/mt-Nd3/mt-Atp6* ("*mt-Genes*") were exported. The expression of all genes significantly changed during development ($p<0.05$; ANOVA, not shown). Transposed data were auto-scaled, and Ward's algorithm was chosen as a clustering method according to Pearson's correlation coefficient distance. Moreover, to assess intersample differences, "heatmaps" were prepared using GenEx or R (Ward's algorithm, Pearson's correlation) with similar results.

Results

mRNA expression microarray data

Gene probes selected for our study were divided into four categories. The first category involved ATPase structural subunits encoded by nuclear DNA (*Atp5a1, Atp5d, Atp5g2, Atp5o*); the second category, ATPase and OXPHOS subunits encoded by mtDNA, generally creating catalytic core of the complex (*mt-Co1, mt-Co2, mt-Nd2, mt-Nd5*, a probe for set of *mt-Co3/mt-Atp8/mt-Nd3/mt-Atp6*); the third ATPase assembly factors (*Atpaf1, Atpaf2, Tmem70*); and the fourth category, other expression regulators involved in mechanism of mitochondrial metabolism acceleration (*Esrra, Nrf1, Gabpa, Ppargc1a, Ppargc1b, Pprc1, Hnf4a* and *Tfam*). Relative expression data from rat expression microarrays were visualized by cluster analysis (Figs 1-3) of these genes in both tissues.

The general appearance of time-course expression curve is in Figure 1. In microarray data, the Pearson's correlation coefficient distance clustering method was used to highlight possible similarities among the expression curve profiles during the five developmental steps (F16, F20, F22, P1 and P4; Figs 2, 3). Pearson's correlation coefficient-based clustering groups mRNA transcripts with remarkably similar expression profiles during the time course of the experiment regardless of the actual amount of the transcript itself. As an appropriate clustering method, Ward's algorithm was chosen, producing tight clusters (other methods – single, complete or average linkage presented similar results). Consistent cluster members in the group regardless of the clustering method were considered significant (Fraley 1998). In liver and skeletal muscle, there were four and three distinct clusters of genes, respectively, throughout development. In liver (L; Fig. 1a), analogous expression profiles were found in clusters: (L1) *Atp5a1, Atp5g2,* and *Atp5o*; (L2) *Tmem70* and *Atpaf1*; (L3) *Atp5d, Nrf1, Atpaf2, Gabpa, Pprc1* and *Tfam*; (L4) *mt-Co1, mt-Co2, mt-Co3/mt-Atp8/mt-Nd3/mt-Atp6, mt-Nd5, Hnf4a, mt-Nd2, Esrra, Ppargc1a* and *Ppargc1b*. In skeletal muscle (M; Fig. 1b), the following were recognized: (M1) *Atp5d, Atp5a1, Atp5g2, Atp5o,*

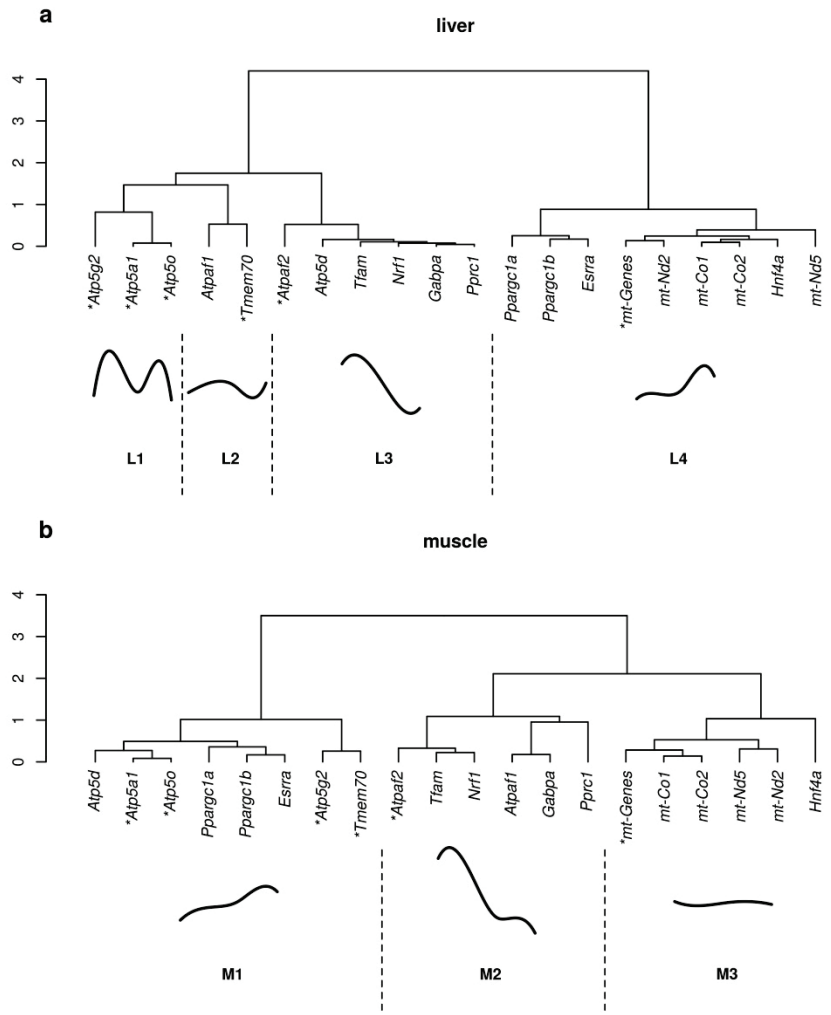

Fig. 1. Overview of microarray data. (**a**) In the liver, twenty genes were divided into four groups according to general expression profile appearance in time (columns from left to right L1-L4). (**b**) In the skeletal muscle, twenty genes were divided into three groups according to general expression profile appearance in time (columns from left to right M1-M3). Asterisks indicate which gene expressions were validated by qPCR. "*mt-Genes*" reflects shared probe for transcripts *mt-Atp6, mt-Atp8, mt-Nd3* and *mt-Co3.*

Ppargc1b, Tmem70, Esrra and *Ppargc1a*; (M2) *Atpaf1, Atpaf2, Gabpa, Nrf1, Pprc1* and *Tfam*; and (M3) *mt-Co1, mt-Co2, mt-Co3/mt-Atp8/mt-Nd3/mt-Atp6, mt-Nd5, mt-Nd2,* and *Hnf4a*. Interestingly, in muscle, there was a stable but mild increase in the expression of some structural ATPase subunits (cluster M1; Figs 1b, 3), whereas the expression of transcription regulators and other OXPHOS subunits decreased (M2) or varied (M3). The only exception is *Tmem70* (M1), the expression of which rose later after birth. In contrast, in liver (Fig. 1a), all structural subunits increased except *Atp5a1, Atp5g2, Atp5o* (L1) and the decreasing *Atp5d* (L3). Moreover, according to cluster analysis, the vast majority of selected regulatory genes in skeletal muscle clustered together (M2), contrary to structural OXPHOS subunits (M1, M3). Although this co-expression tendency was not observed in liver, it could be noted that some smaller groups of genes were found in both tissues regardless of the tissue type, specifically *Atp5a1, Atp5o,* and *Atp5g2* (L1, M1); *mt-Co1, mt-Co2,* and *mt-Co3/mt-Atp8/mt-Nd3/mt-Atp6* (L4, M3); *Ppargc1a* and *Ppargc1b* (L4, M1); and *Atpaf2, Nrf1, Gabpa, Tfam,* and *Pprc1* (L3, M2).

"Heatmap" cluster analysis (Figs 2, 3) showed that samples of the same age have highly similar expression patterns in both tissues (except sample E from F22 day, F22e, Fig. 3). In contrast, in the liver, we defined two groups with significantly different expression patterns corresponding to the actual state of development. The first group consisted of samples F20 and younger, and the second of samples F22 and older (both prenatal and postnatal; Fig. 2). In skeletal muscle, only F16 samples had dissimilar expression patterns to F20 or older individuals (Fig. 3).

mRNA quantification by qPCR

To more precisely assess both the expression level and pattern of some ATPase subunits and assembly factors, qPCR was performed in at least four or more rat individuals per each fetal/postnatal day (F16-22, P1-5; Fig. 4).

In liver fetal mRNA expression generally stayed low, in contrast to diverse expression levels in fetal

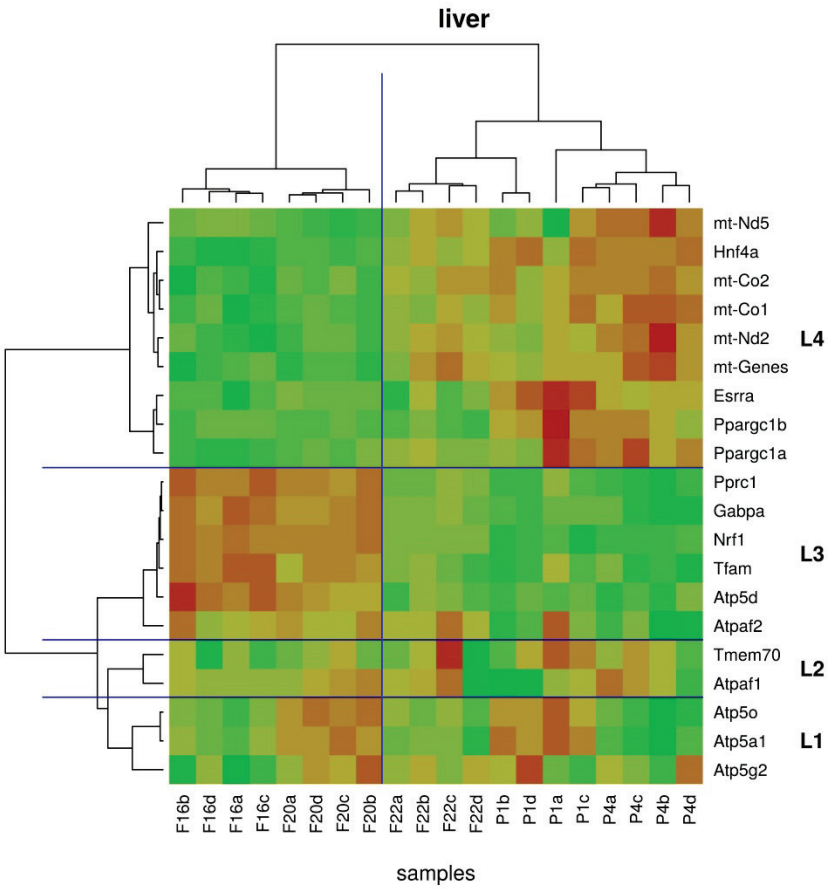

Fig. 2. Heatmap clustering (liver samples). Genes and samples were clustered according Pearson correlation coefficient distance. Left dendrogram shows clusters L1-L4 (from Fig. 1a) separated by horizontal blue lines. Upper dendrogram shows intersample variability. Samples can be identified by the letters a-d (individual littermate) and age (fetal 16-22 in days post conception F16-22; postnatal 1-4 in days after birth P1-4). All samples can be divided into two groups (separated by vertical blue line) – early fetal (F16a-F20d) and late fetal/early postnatal (F22a-P4d). "*mt-Genes*" reflects shared probe for transcripts *mt-Atp6, mt-Atp8, mt-Nd3* and *mt-Co3*.

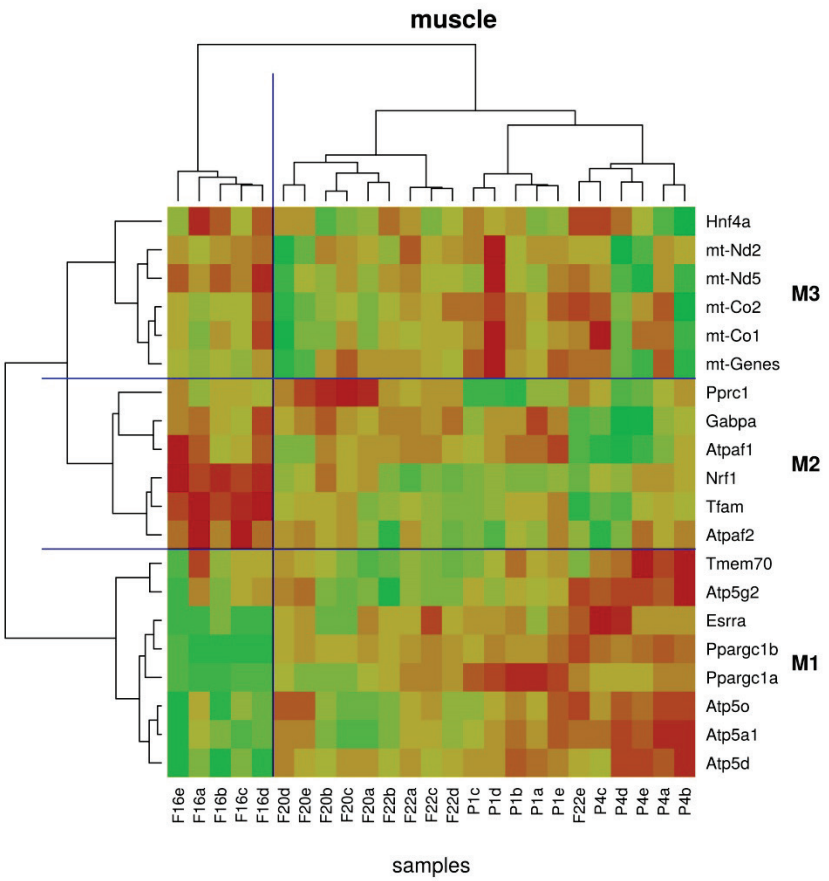

Fig. 3. Heatmap clustering (skeletal muscle samples). Genes and samples were clustered according Pearson correlation coefficient distance. Left dendrogram shows clusters M1-M3 (from Fig. 1b) separated by horizontal blue lines. Upper dendrogram shows intersample variability. Samples can be identified by the letters a-e (individual littermate) and age (fetal 16-22 in days post conception F16-22; postnatal 1-4 in days after birth P1-4). Only samples F16a-F16e have different expression pattern (separated by vertical blue line) compared to the riper fetal/early postnatal samples (F20-P4). "*mt-Genes*" reflects shared probe for transcripts *mt-Atp6, mt-Atp8, mt-Nd3* and *mt-Co3*.

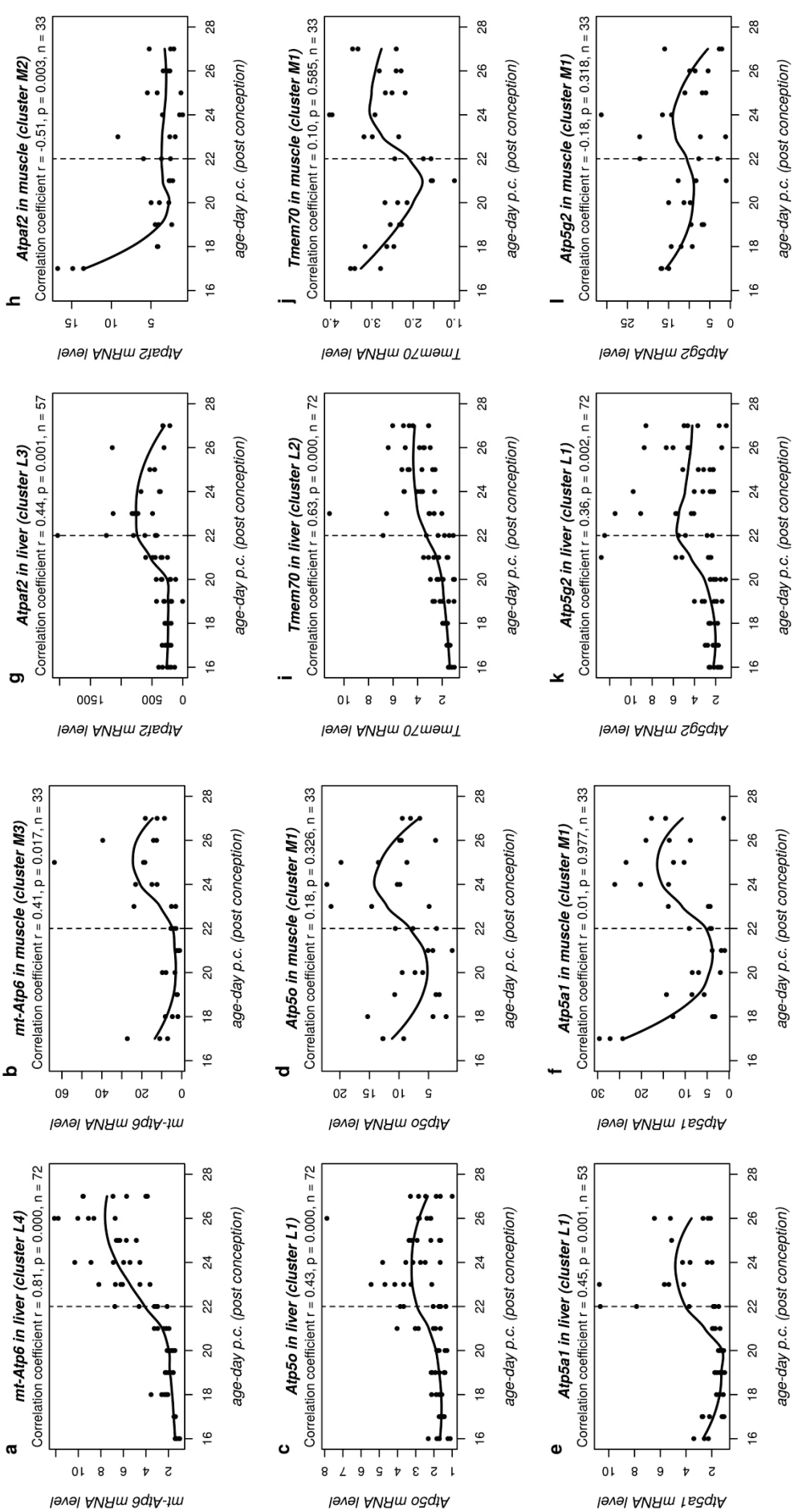

Fig. 4. (a-f): qPCR of *mt-Atp6* (**a**, **b**), *Atp5o* (**c**, **d**), *Atp5a1* (**e**, **f**) in both liver and skeletal muscle samples. Clusters L1-L4 and M1-M3 according to Figs 1-3 are indicated. Significant increase/decrease ($p<0.05$) is shown in each graph (Table 1). The dashed line indicates the last fetal day/birth. **(g-l)**: qPCR of *Atpaf2* (**g**, **h**), *Tmem70* (**i**, **j**) and *Atp5g2* (**k**, **l**) in both liver and skeletal muscle samples. Clusters L1-L4 and M1-M3 according to Figs 1-3 are indicated. Significant increase/decrease ($p<0.05$) is shown in each graph (Table 1). The dashed line indicates the last fetal day/birth.

skeletal muscle (Fig. 4). After birth, the majority of expression patterns in both tissues showed an important shift: mRNA quantity rose. An overall increasing expression trend was significant in *Atp5g2, Atp5o, mt-Atp6, Atpaf2, Atp5a1* and *Tmem70* in liver (Fig. 4a, c, e, g, i, k) but only *mt-Atp6* and *Atpaf2* in muscle (Fig. 4b, h). Moreover, in muscle, *Atpaf2* expression significantly decreased during the perinatal period. All statistics from qPCR data are summarized in Table 1 together with the number of analyzed samples, correlation coefficient and p-value of significant trend changes.

In the liver, the *mt-Atp6* (cluster L4; Figs 2, 4a) expression profile showed massively increased mRNA levels starting approximately at the 22nd gestational day. The highest expression was acquired at the 4th postnatal day. *Atp5o, Atp5a1* and *Atp5g2* (L1; Figs 2, 4c, e, k) had a different progression; earlier in development, the expression of these genes was quite stable, with an increase between the 21st and 22nd gestational day, but immediately after birth, expression began to slowly diminish. *Tmem70* expression (L2; Figs 2, 4i) demonstrated a mild increase before birth, with higher expression after parturition when the expression level stabilized. In contrast, *Atpaf2* (L3; Figs 2, 4g) was a differentially expressed assembly factor, as it showed a very stable expression level prenatally and peak of high expression between the 21st gestational and first postnatal day with an ongoing decrease to fetal levels by the 4th postnatal day.

In skeletal muscle, we observed a higher similarity along the course of expression. *mt-Atp6* (M3; Figs 3, 4b), *Atp5a1* (M1; Figs 3, 4f) and *Tmem70* (M1; Figs 3, 4j) all exhibited an analogous expression trend. Higher expression levels at the 16th day of gestation declined to very low levels between the 19th and 22nd gestational day. After birth, a transient increase in expression occurred. Additionally, *Atp5o* (M1; Figs 3, 4d) and *Atp5g2* (M1; Figs 3, 4l) had similar expression profiles, but the trend was not significant. As in the liver, *Atpaf2* had the most specific expression profile among other genes (M2; Figs 3, 4h). *Atpaf2* expression dramatically decreased between the 17th and 19th gestational days. Afterwards, the expression level was stabilized throughout the next three days of fetal development and the entire postnatal period.

Overall, between both tissues, the expression profiles of mRNA transcripts were quite different. For example, *Atp5o* in liver (Fig. 4c) shows almost no change prenatally with a significant increase in the neonatal period; in contrast, in skeletal muscle, the *Atp5o* (Fig. 4d) expression level decreases approaching birth; however, its general expression trend remained statistically insignificant. However, the peak expression shift at the first and second postnatal day seemed to occur more generally.

Another aspect to note was that not all genes that were indicated to significantly change expression according to microarray data results appeared significantly changed by qPCR analysis. This discrepancy is an example of the crucial nature of microarray data validation.

Protein analysis

To assess the present ATPase content in the developing rat tissue ATPase α subunit (Atp5a), immunodetection by Western blot was performed. Due to high variability in common reference loading protein amounts (GAPDH, β-actin, α-tubulin and others), Hprt was used as a reference loading protein (also used for qPCR data normalization). It was shown that the relative quantity of the ATPase α subunit is slightly higher in postnatal tissues (Fig. 5) compared to prenatally obtained samples. Unfortunately, a reliable reference protein for sample loading normalization is missing, making protein analysis challenging.

Discussion

Mitochondrial biogenesis has been previously studied on both transcriptional and functional levels in mice and rats (Cuezva *et al.* 1997), but mainly postnatally. Studies showing expression changes during mitochondrial biogenesis on a fewer distinct genes, e.g. *ATP5B* (Izquierdo and Cuezva 1997, Izquierdo *et al.* 1990, 1995) were published. Other study shows co-expression of 13 transcripts out of 16 cytochrome *c* oxidase mRNAs (Kim *et al.* 1995). Finally, mitochondrial biogenesis was studied in prenatal human liver and muscle (Pejznochova *et al.* 2010) from abortions indicated due to non-mitochondrial-disease reasons. Our presented work is based on microarray and qPCR data from rat tissues obtained during the both late prenatal and early postnatal (perinatal) period and highlights expression characteristics common for this period and orchestration of expression of 20 mitochondria-related genes (ATPase subunits, mitochondrial-metabolism regulators). Unique to the tissue determination, skeletal muscle was chosen as a model tissue, the function of which stays generally unchanged throughout early

mammalian ontogenesis. Contrary to skeletal muscle, liver was chosen as a model tissue with special variable functions. During the fetal period, liver plays a role not only in hematopoiesis, which should change after birth when hematopoiesis moves to bone marrow (Mikkola and Orkin 2006), but also in other metabolic pathways (e.g., fatty acids β-oxidation), which are promoted during this period (Herrera 2000).

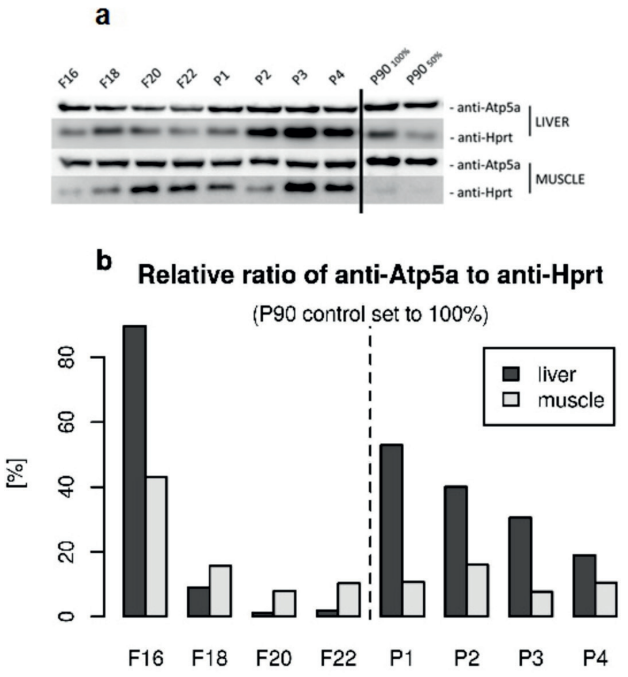

Fig. 5. Immunodetection of Atp5a and reference Hprt in the liver and the skeletal muscle (SDS/PAGE, Western blot) and signal quantification. (**a**) Western blot was performed in duplicate. Expression of Atp5a in the skeletal muscle was stable, whereas in the liver, a slight increase in Atp5a content was observed. (**b**) Quantification of chemiluminescence signal was performed twice per each replicate (membrane), and the average is presented as % of 90-day-old adult control signal ratio of anti-Atp5a to anti-Hprt antibody (P90 100 % or 50 % loading means 20 or 10 ng of protein per well, respectively). The dashed line indicates the last fetal day/birth.

Microarray expression data of ATPase- and mitochondria-related genes enabled us to obtain an overview into possible expression interconnections characteristic of the late fetal and early postnatal periods. These data might be useful for identification of factors playing role in the earlier postulated hypothesis about post-transcription regulation of mitochondrial mRNAs (Izquierdo and Cuezva 1997) and the role of translation inhibition proteins or small RNAs (Willers *et al.* 2012) in the preparation of the fetus for transition to extra-uterine conditions.

Overall, more extensive changes (over two-fold) were observed in the liver. In muscle, expression was more stable, in agreement with our initial premise of stable skeletal muscle function throughout early mammalian development. However, the main transcriptional regulators, *Nrf1* and *Gabpa*, were expressed in an analogous manner in both tissues, indicating that a pivotal regulation is dependent on tissue-specific regulators (e.g. *Hnf4a*).

To assess intersample variations, we created expression "heatmaps" showing tight gene expression similarities between samples of the same age. Moreover, we predicted a possible metabolic switch on the transcriptional level that occurred in the liver after F20 (the reversal of the higher expression levels of transcriptional regulators and the acceleration of the expression of structural subunits) i.e., before birth (Figs 2, 3). Based on this observation, we assume that the fetus undergoes key liver expression reprogramming about two days before the actual birth, which may help stimulate adequate adaptation to external conditions. We hypothesize that these expression changes are driven by multiple triggers, including estrogen (Rosenthal *et al.* 2004) or other hormones, that increase during pregnancy and labor (Smith *et al.* 2009) and interact with both transcription factors (e.g., estrogen receptors) or ATPase itself (Moreno *et al.* 2013). In skeletal muscle, only F16 samples had significantly different expression patterns. This is likely due to skeletal muscle immaturity, not a metabolic switch affected by functional or physiological development, considering that muscle fiber formation starts at F15, fiber type differentiation is initiated after F17 (Rubinstein and Kelly 1981) and major differentiation and metabolic shift occurs later during the time of weaning (Punkt *et al.* 2004). Nevertheless, further experiments must be performed on premature neonates to verify this interpretation.

ATPase biogenesis has mainly been studied in *S. cerevisiae* (Ackerman and Tzagoloff 2005, Rak *et al.* 2011). Not all homologues of yeast subunits and assembly factors are present in mammalian cells, but we propose that structural OXPHOS subunits show higher expression similarity in the specific curve pattern, especially for mtDNA-encoded genes (Fig. 1a, b), the expression of which is accelerated after birth. This process might be explained by the saturation of subunits added in the last steps of ATPase biogenesis (Wittig *et al.* 2010). In contrast, lower expression of *Atp5o* or *Atp5g2* indicates possible rate-limiting subunits of ATPase

biogenesis, which might serve as structural scaffolds for subsequent subunits (Houstěk *et al.* 1995, Straffon *et al.* 1998). Moreover, lower and tissue-specific *Atpaf2* expression predicts its enhancement role in ATPase activity in liver very early after birth. Similarly, Tmem70 has a non-essential assembly role in the liver that is crucial later after birth, when higher ATP demands are needed. This role might clarify why *Tmem70* expression stably increases over more than 4 days of life. This increase corresponds with non-zero ATPase activities and approximately 30 % ATPase concentrations in patients with homozygous mutations/deletions in *TMEM70* who suffer from ATPase deficiency and have adverse clinical findings with identical mitochondrial disorder (Cízková *et al.* 2008, Spiegel *et al.* 2011).

Recently, probably a key regulator of *ATP5B* translation was described, miR-127-5p (Willers *et al.* 2012), and we believe, that presented data, which describe expression of other ATPase-related genes, may serve as a valid background for finding more factors, which start the preparation of the fetus for the transition to extrauterine conditions.

Finally, our study supports the crucial nature of the qPCR validation of microarray data. Although we found a prenatal expression switch in the vast majority of the 20 selected genes (e.g., *Tmem70* in muscle, *Atp5a1*), not all results were consistent (e.g., minor changes of *Atp5o* or *Atp5g2* on microarray and significant changes quantified by qPCR). Still, subsequent qPCR or immunodetection data validation represents a gold standard.

Conclusions

In this study, we present a brief characterization of complex microarray data in user-friendly graphical software, which might be useful for analyzing microarray data in the broader context of cell metabolism and physiology during ontogenetic development. Moreover, a unique expression correlation among mtDNA-encoded ATPase and OXPHOS subunits and mitochondrial biogenesis regulators were shown in both liver and skeletal muscle tissue during the rat fetal-to-neonatal transition. The group of Cuezva *et al.* (1997) published the hypothesis that organized coexpression of mitochondrial mRNAs, the mRNA translation efficiency and mRNA stability are crucial for postnatal adaptation of newborn mammal. From our data, in correlation with this previous hypothesis, we can say that in rat liver a key expression reprogramming occurs about two days before birth. We might hypothesize that in mammals (including humans) this period might determine specific critical gestational age of preterm neonates associated with early neonatal morbidity and mortality arising from mitochondrial-metabolism insufficiency. Although precise identification of this period remains to be elucidated by further research studies, we believe that these findings will be useful for further improvement in diagnostics of congenital metabolic disorders connected with mitochondrial deficiency or newborn prematurity.

Conflict of Interest

There is no conflict of interest.

Acknowledgements

We would like to thank Dr. Michal Pravenec and Dr. Petr Mlejnek from Department of Genetics and Model Diseases, Institute of Physiology, Academy of Sciences of the Czech Republic, Prague for obtaining and providing rat tissue samples for this project. This study was supported by research grant of Charles University Grant Agency (GAUK), No. 667612, First Faculty of Medicine, Charles University in Prague; Grant Agency of Czech Republic, GACR 14-36804G, Centre of mitochondrial biology and pathology (MITOCENTRE); UNCE 204011 and PRVOUK P24/205024-4.

References

"R Core Team" URL: http://www.r-project.org/: R: A language and environment for statistical computing. 2014.

ACKERMAN SH, TZAGOLOFF A: Function, structure, and biogenesis of mitochondrial ATP synthase. *Prog Nucleic Acid Res Mol Biol* **80**: 95-133, 2005.

BENARD G, FAUSTIN B, PASSERIEUX E, GALINIER A, ROCHER C, BELLANCE N, DELAGE JP, CASTEILLA L, LETELLIER T, ROSSIGNOL R: Physiological diversity of mitochondrial oxidative phosphorylation. *Am J Physiol Cell Physiol* **291**: C1172-C1182, 2006.

BOYER PD: A model for conformational coupling of membrane potential and proton translocation to ATP synthesis and to active transport. *FEBS Lett* **58**: 1-6, 1975.

BURCH HB, LOWRY OH, KUHLMAN AM, SKERJANCE J, DIAMANT EJ, LOWRY SR, VON DIPPE P: Changes in patterns of enzymes of carbohydrate metabolism in the developing rat liver. *J Biol Chem* **238**: 2267-2273, 1963.

CÍZKOVÁ A, STRÁNECKÝ V, MAYR JA, TESAROVÁ M, HAVLÍCKOVÁ V, PAUL J, IVÁNEK R, KUSS AW, HANSÍKOVÁ H, KAPLANOVÁ V, VRBACKÝ M, HARTMANNOVÁ H, NOSKOVÁ L, HONZÍK T, DRAHOTA Z, MAGNER M, HEJZLAROVÁ K, SPERL W, ZEMAN J, HOUSTEK J, KMOCH S: TMEM70 mutations cause isolated ATP synthase deficiency and neonatal mitochondrial encephalocardiomyopathy. *Nat Genet* **40**: 1288-1290, 2008.

CUEZVA JM, OSTRONOFF LK, RICART J, LÓPEZ DE HEREDIA M, DI LIEGRO CM, IZQUIERDO JM: Mitochondrial biogenesis in the liver during development and oncogenesis. *J Bioenerg Biomembr* **29**: 365-377, 1997.

FORNUSKOVA D, BRANTOVA O, TESAROVA M, STIBUREK L, HONZIK T, WENCHICH L, TIETZEOVA E, HANSIKOVA H, ZEMAN J: The impact of mitochondrial tRNA mutations on the amount of ATP synthase differs in the brain compared to other tissues. *Biochim Biophys Acta* **1782**: 317-325, 2008.

FRALEY C: Algorithms for model-based Gaussian hierarchical clustering. *Siam J Sci Comput* **20**: 270-281, 1998.

HERRERA E: Metabolic adaptations in pregnancy and their implications for the availability of substrates to the fetus. *Eur J Clin Nutr* **54** (Suppl 1): S47-S51, 2000.

HOUSTĚK J, ANDERSSON U, TVRDÍK P, NEDERGAARD J, CANNON B: The expression of subunit c correlates with and thus may limit the biosynthesis of the mitochondrial F_0F_1-ATPase in brown adipose tissue. *J Biol Chem* **270**: 7689-7694, 1995.

IZQUIERDO JM, CUEZVA JM: Control of the translational efficiency of beta-F1-ATPase mRNA depends on the regulation of a protein that binds the 3' untranslated region of the mRNA. *Mol Cell Biol* **17**: 5255-5268, 1997.

IZQUIERDO JM, LUIS AM, CUEZVA JM: Postnatal mitochondrial differentiation in rat liver. Regulation by thyroid hormones of the beta-subunit of the mitochondrial F1-ATPase complex. *J Biol Chem* **265**: 9090-9097, 1990.

IZQUIERDO JM, RICART J, OSTRONOFF LK, EGEA G, CUEZVA JM: Changing patterns of transcriptional and post-transcriptional control of beta-F1-ATPase gene expression during mitochondrial biogenesis in liver. *J Biol Chem* **270**: 10342-10350, 1995.

KIM K, LECORDIER A, BOWMAN LH: Both nuclear and mitochondrial cytochrome c oxidase mRNA levels increase dramatically during mouse postnatal development. *Biochem J* **306**: 353-358, 1995.

LENAZ G, GENOVA ML: Kinetics of integrated electron transfer in the mitochondrial respiratory chain: random collisions vs. solid state electron channeling. *Am J Physiol Cell Physiol* **292**: C1221-C1239, 2007.

LENAZ G, GENOVA ML: Structural and functional organization of the mitochondrial respiratory chain: a dynamic super-assembly. *Int J Biochem Cell Biol* **41**: 1750-1772, 2009.

LOWRY OH, ROSEBROUGH NJ, FARR AL, RANDALL RJ: Protein measurement with the Folin phenol reagent. *J Biol Chem* **193**: 265-275, 1951.

MIKKOLA HK, ORKIN SH: The journey of developing hematopoietic stem cells. *Development* **133**: 3733-3744, 2006.

MINAI L, MARTINOVIC J, CHRETIEN D, DUMEZ F, RAZAVI F, MUNNICH A, RÖTIG A: Mitochondrial respiratory chain complex assembly and function during human fetal development. *Mol Genet Metab* **94**: 120-126, 2008.

MORENO AJ, MOREIRA PI, CUSTODIO JB, SANTOS MS: Mechanism of inhibition of mitochondrial ATP synthase by 17β-estradiol. *J Bioenerg Biomembr* **45**: 261-270, 2013.

PEJZNOCHOVÁ M, TESAROVÁ M, HONZÍK T, HANSÍKOVÁ H, MAGNER M, ZEMAN J: The developmental changes in mitochondrial DNA content per cell in human cord blood leukocytes during gestation. *Physiol Res* **57**: 947-955, 2008.

PEJZNOCHOVA M, TESAROVA M, HANSIKOVA H, MAGNER M, HONZIK T, VINSOVA K, HAJKOVA Z, HAVLICKOVA V, ZEMAN J: Mitochondrial DNA content and expression of genes involved in mtDNA transcription, regulation and maintenance during human fetal development. *Mitochondrion* **10**: 321-329, 2010.

PRYSTOWSKY H: Fetal blood studies. VII. The oxygen pressure gradient between the maternal and fetal bloods of the human in normal and abnormal pregnancy. *Bull Johns Hopkins Hosp* **101**: 48-56, 1957.

PUNKT K, NAUPERT A, ASMUSSEN G: Differentiation of rat skeletal muscle fibres during development and ageing. *Acta Histochem* **106**: 145-154, 2004.

RAK M, GOKOVA S, TZAGOLOFF A: Modular assembly of yeast mitochondrial ATP synthase. *EMBO J* **30**: 920-930, 2011.

ROSENTHAL M, ALBRECHT E, PEPE G: Estrogen modulates developmentally regulated gene expression in the fetal baboon liver. *Endocrine* **23**: 219-228, 2004.

RUBINSTEIN NA, KELLY AM: Development of muscle fiber specialization in the rat hindlimb. *J Cell Biol* **90**: 128-144, 1981.

SCHÄGGER H, PFEIFFER K: The ratio of oxidative phosphorylation complexes I-V in bovine heart mitochondria and the composition of respiratory chain supercomplexes. *J Biol Chem* **276**: 37861-37867, 2001.

SCHÄGGER H, VON JAGOW G: Tricine-sodium dodecyl sulfate-polyacrylamide gel electrophoresis for the separation of proteins in the range from 1 to 100 kDa. *Anal Biochem* **166**: 368-379, 1987.

SMITH R, SMITH JI, SHEN X, ENGEL PJ, BOWMAN ME, MCGRATH SA, BISITS AM, MCELDUFF P, GILES WB, SMITH DW: Patterns of plasma corticotropin-releasing hormone, progesterone, estradiol, and estriol change and the onset of human labor. *J Clin Endocrinol Metab* **94**: 2066-2074, 2009.

SPIEGEL R, KHAYAT M, SHALEV SA, HOROVITZ Y, MANDEL H, HERSHKOVITZ E, BARGHUTI F, SHAAG A, SAADA A, KORMAN SH, ELPELEG O, YATSIV I: TMEM70 mutations are a common cause of nuclear encoded ATP synthase assembly defect: further delineation of a new syndrome. *J Med Genet* **48**: 177-182, 2011.

STRAFFON AF, PRESCOTT M, NAGLEY P, DEVENISH RJ: The assembly of yeast mitochondrial ATP synthase: subunit depletion in vivo suggests ordered assembly of the stalk subunits b, OSCP and d. *Biochim Biophys Acta* **1371**: 157-162, 1998.

SUTTON R, POLLAK JK: The increasing adenine nucleotide concentration and the maturation of rat liver mitochondria during neonatal development. *Differentiation* **12**: 15-21, 1978.

VALCARCE C, NAVARRETE RM, ENCABO P, LOECHES E, SATRÚSTEGUI J, CUEZVA JM: Postnatal development of rat liver mitochondrial functions. The roles of protein synthesis and of adenine nucleotides. *J Biol Chem* **263**: 7767-7775, 1988.

WANG ZG, WHITE PS, ACKERMAN SH: Atp11p and Atp12p are assembly factors for the F(1)-ATPase in human mitochondria. *J Biol Chem* **276**: 30773-30778, 2001.

WILLERS IM, MARTÍNEZ-REYES I, MARTÍNEZ-DIEZ M, CUEZVA JM: miR-127-5p targets the 3'UTR of human β-F1-ATPase mRNA and inhibits its translation. *Biochim Biophys Acta* **1817**: 838-848, 2012.

WITTIG I, MEYER B, HEIDE H, STEGER M, BLEIER L, WUMAIER Z, KARAS M, SCHÄGGER H: Assembly and oligomerization of human ATP synthase lacking mitochondrial subunits a and A6L. *Biochim Biophys Acta* **1797**: 1004-1011, 2010.